Supplementary Information for

Vehicle Induced Turbulence and Atmospheric Pollution

Paul A. Makar, Craig Stroud, Ayodeji Akingunola, Junhua Zhang, Shuzhan Ren, Philip Cheung, Qiong Zheng

Paste corresponding author name here
Email: paul.makar@canada.ca

This PDF file includes:

Supplementary text to Figure S5
Figures S1 to S13
Tables S1

Supplementary Information Text

Statistics used for model evaluation

The formulae for the standard statistical metrics used here for model performance evaluation, their abbreviations, description, and the value of a perfect model score, appear in Table S1. Model values for evaluation were taken from the lowest model layer in the grid cell closest to the surface monitoring network observation points (nearest neighbor approach; no interpolation of model values).

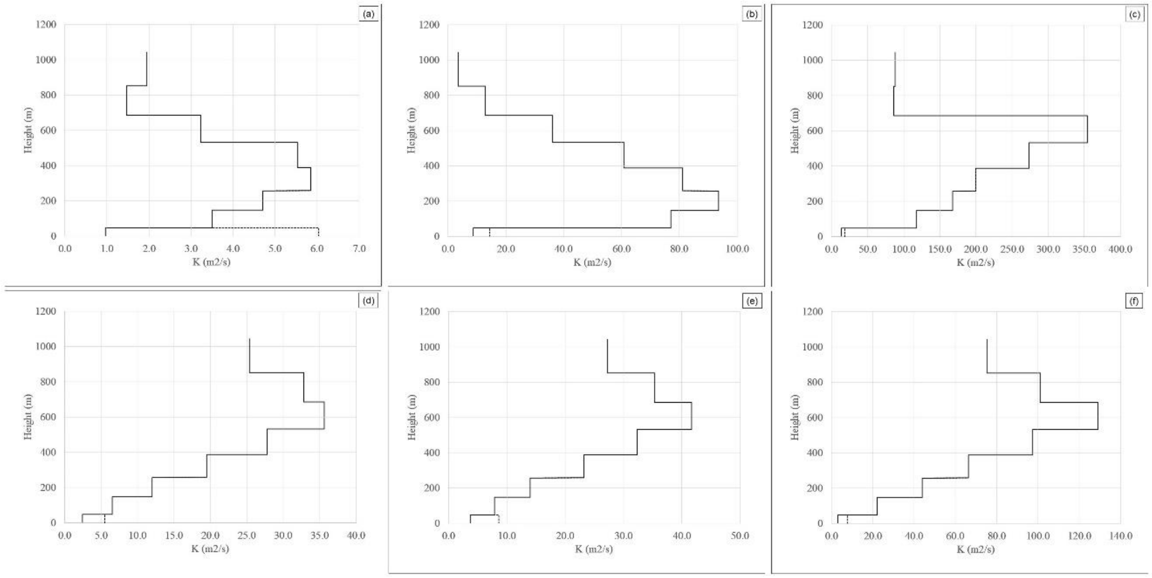

Fig. S1. : Comparison of average *K* (solid line) and *K* + K_{VIT} (dashed line), for Manhattan Island grid cell, 2.5km resolution simulations. (a) July, 10 UT (6 AM EDT), (b) July 14 UT (10 AM EDT), (c) July, 22 UT (6 PM EDT), (c) January, 10 UT (6 AM EST), (d) January, 14 UT (10 AM EST), (e) January, 22 UT (6 PM EST).

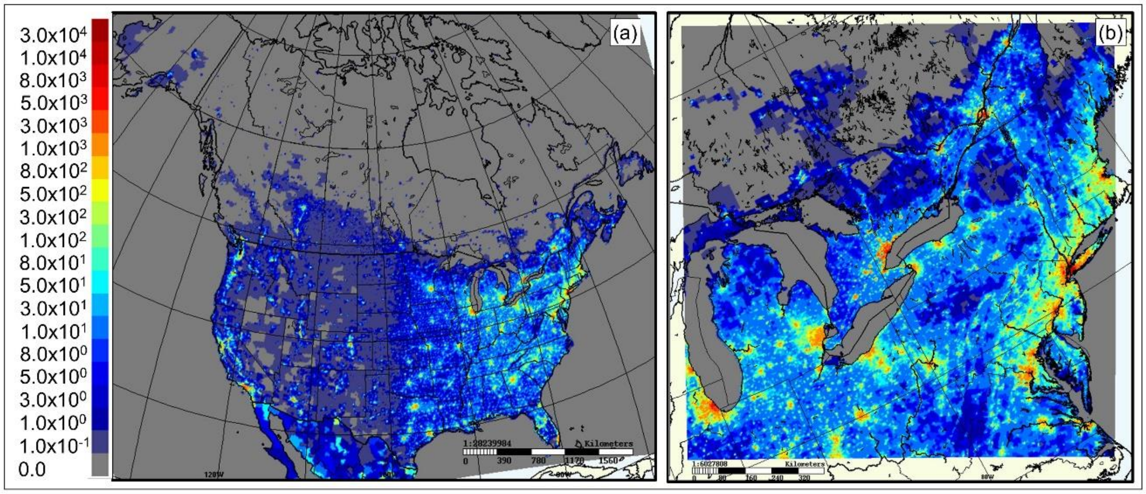

Fig. S2. Population density (km^{-2}) for (a) North American 10km grid cell size; (b) High Resolution 2.5km grid cell size domains.

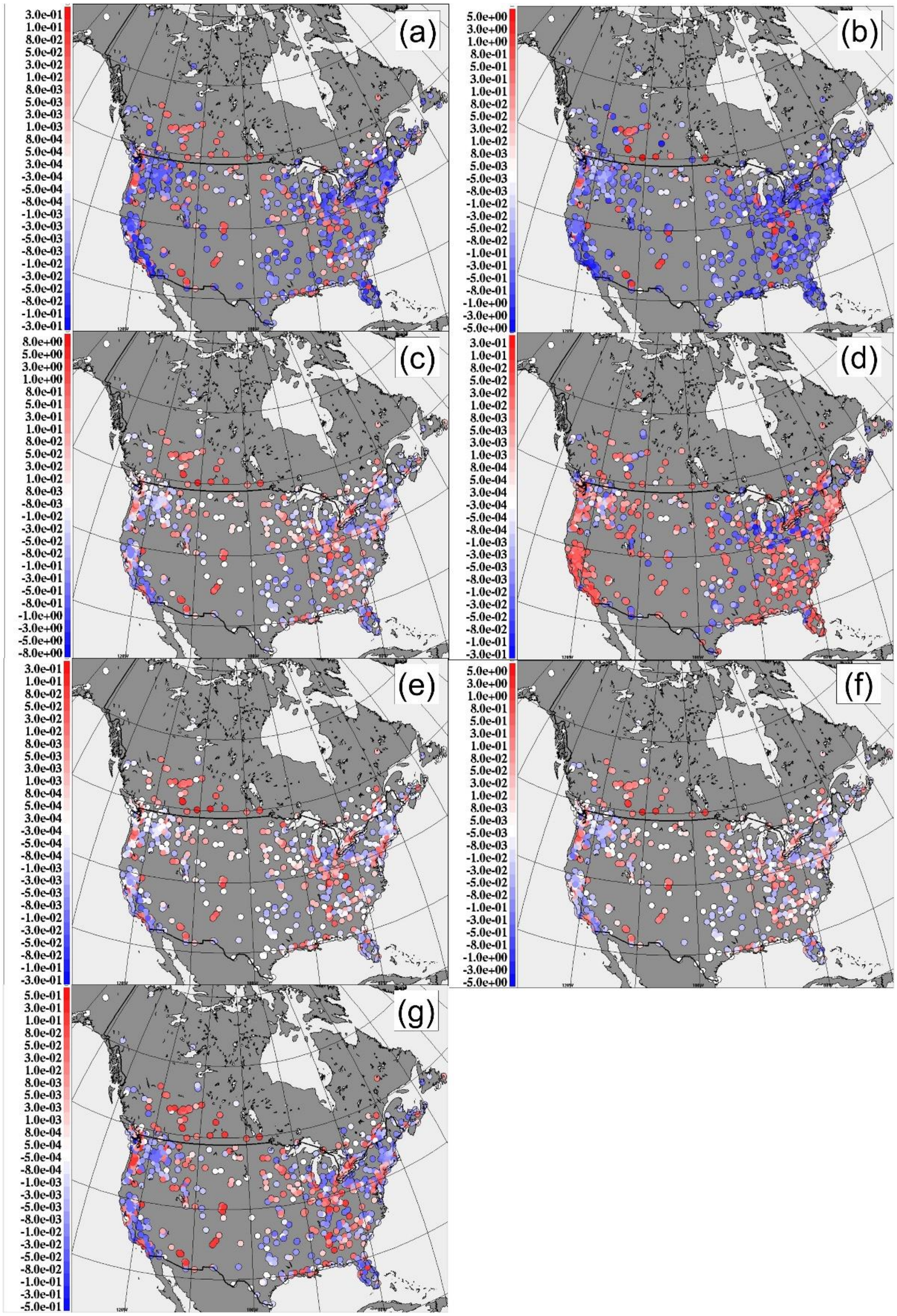

Fig. S3. Change in model PM2.5 performance at 943 North American surface monitoring sites, July 2016 ($\mu g\ m^{-3}$). Red colours indicate stations where the addition of the VIT parameterization improved model performance, blue colours indicate stations where the addition of the VIT parameterization degraded model performance. (a) $\Delta FAC2_{VIT-No\ VIT}$; (b) $\Delta|MB|_{No\ VIT-VIT}$; (c) $\Delta MGE_{No\ VIT-VIT}$; (d) $\Delta r_{VIT-No\ VIT}$; (e) $\Delta RMSE_{No\ VIT-VIT}$; (f) $\Delta COE_{VIT-No\ VIT}$; (g) $\Delta IOA_{VIT-No\ VIT}$.

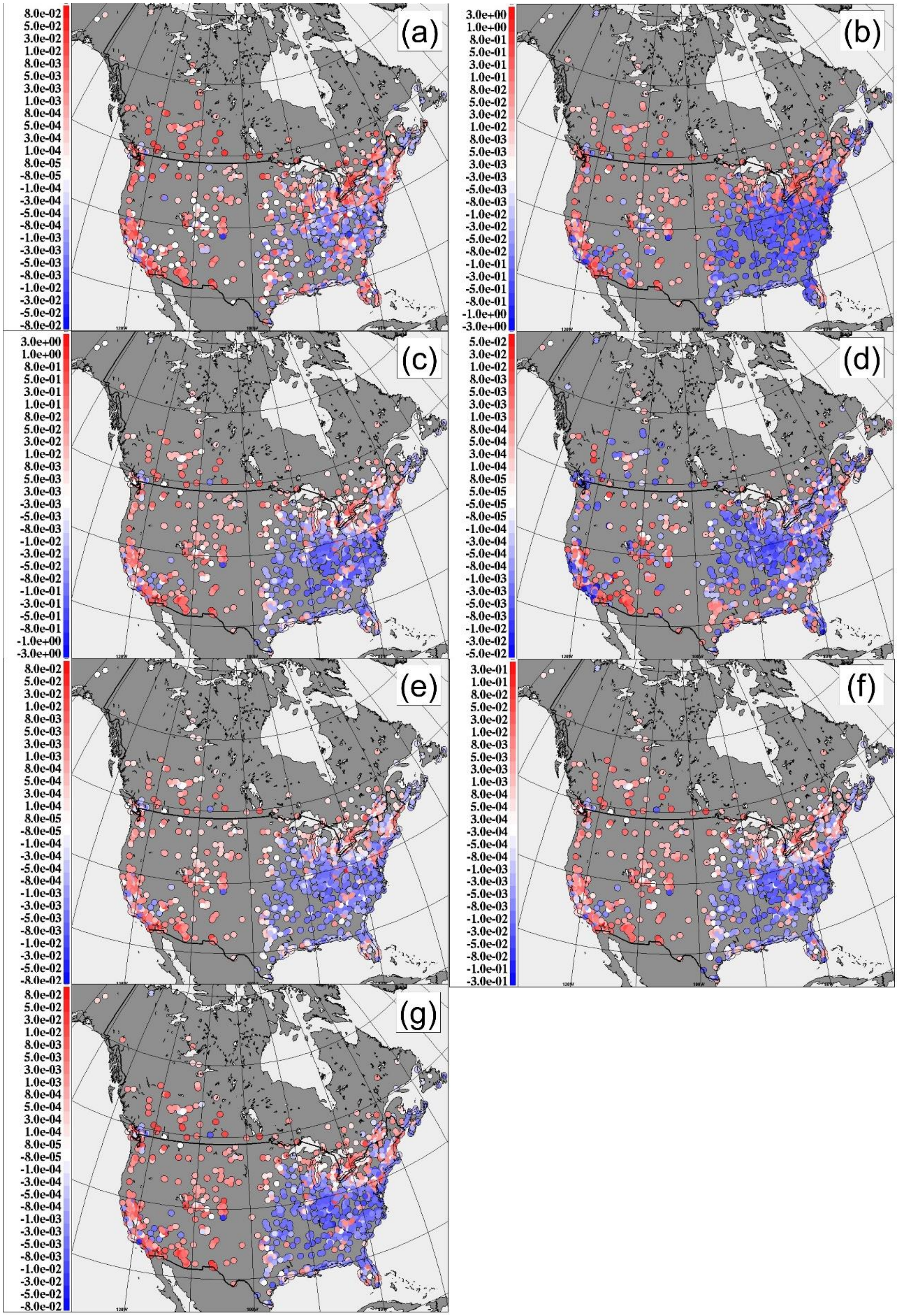

Fig. S4. Change in model O_3 performance at 1384 North American surface monitoring sites, July 2016 (ppbv). Colours and panel labels as in Figure S4.

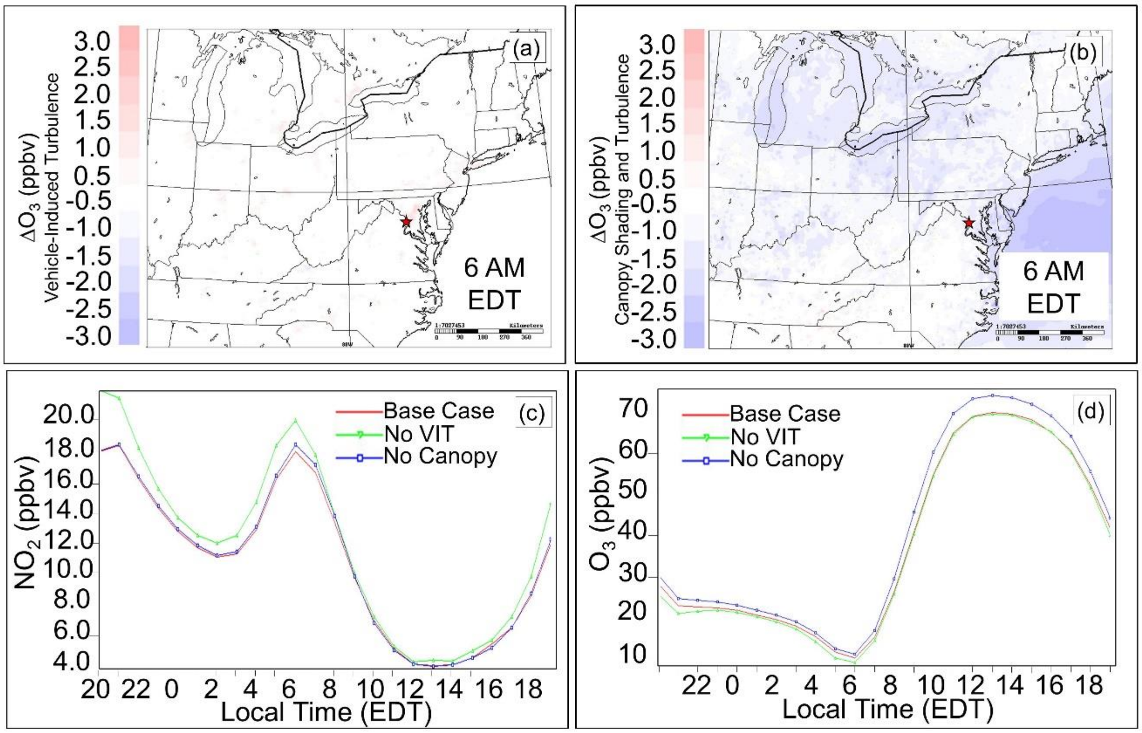

Fig. S5. Change in model NO_2 and O_3 for the months of July, August and September of 2016 associated with VIT and forest canopy turbulence. (a) Change in average surface O_3 due to vehicle-induced turbulence at 6 AM local time. Note small increases (pink) in urban areas. (b) Change in average O_3 due to reduced turbulence and shading within forested canopies (blue). (c) Changes in average NO_2 concentration in Washington, D.C. associated with removing the VIT and forest canopy parameterizations. (d) Changes in average O_3 concentration associated with removing the VIT and forest canopy parameterizations.

Our main text focusses on the impact of vehicle-induced turbulence relative to a simulation containing neither VIT nor the effects of forest canopy shading and turbulence. Here, we briefly discuss the effects of *combining* these two parameterizations, using a set of three July-August-September 2016 simulations.

The details of the forest canopy shading and turbulence parameterization are discussed elsewhere (Makar et al., 2017). Briefly, this parameterization accounts for the reduction in turbulent kinetic energy and in photolysis rates associated forest canopies. In this parameterization, three additional vertical layers are added to below the canopy height, turbulence is decreased to account for lower TKE values below the canopy height, and the shading due to foliage (a function of canopy height, leaf area index, and clumping index) is used to reduce photolysis rates. The reader is directed to Makar et al (2017) for the observational basis and mathematical description underlying this parameterization.

Figure S5(a) shows the effect of VIT on July-August-September average O_3 concentrations at 6 AM local time. Small increases in O_3 concentrations occur, in the urban areas, due to the reduction in NOx titration in the early morning hours resulting from VIT. These increases in O_3 are on the order of 0.5 ppbv or less (light pink shades). Figure S5(b) shows the effect of forest canopy turbulence and shading on O_3 concentrations in the same region; decreases in average O_3 over the region of up to 3 ppbv. Combined, the canopy turbulence and shading has a stronger impact on O_3 biases than vehicle-induced turbulence. Figure S5(c) shows the hourly average NO_2 concentrations in Washington DC for three simulations: a base case (red line) which includes both VIT and forest canopy effects, and two scenarios, in which the VIT parameterization (green line) and the forest canopy parameterization (blue line) are removed. The VIT parameterization is responsible for a nighttime and early morning NO_2 reduction of about 2 ppbv (going from green to red lines), while the canopy parameterization has minimal impact on urban NO_2. Figure S5(d) shows the corresponding average O_3 time series; the VIT parameterization results in a small nighttime increase in O_3 (going from green to red line), but this is offset when forest canopy effects are included; the latter are also responsible for reducing the average daytime O_3 by about 5 ppbv (going from blue to red lines).

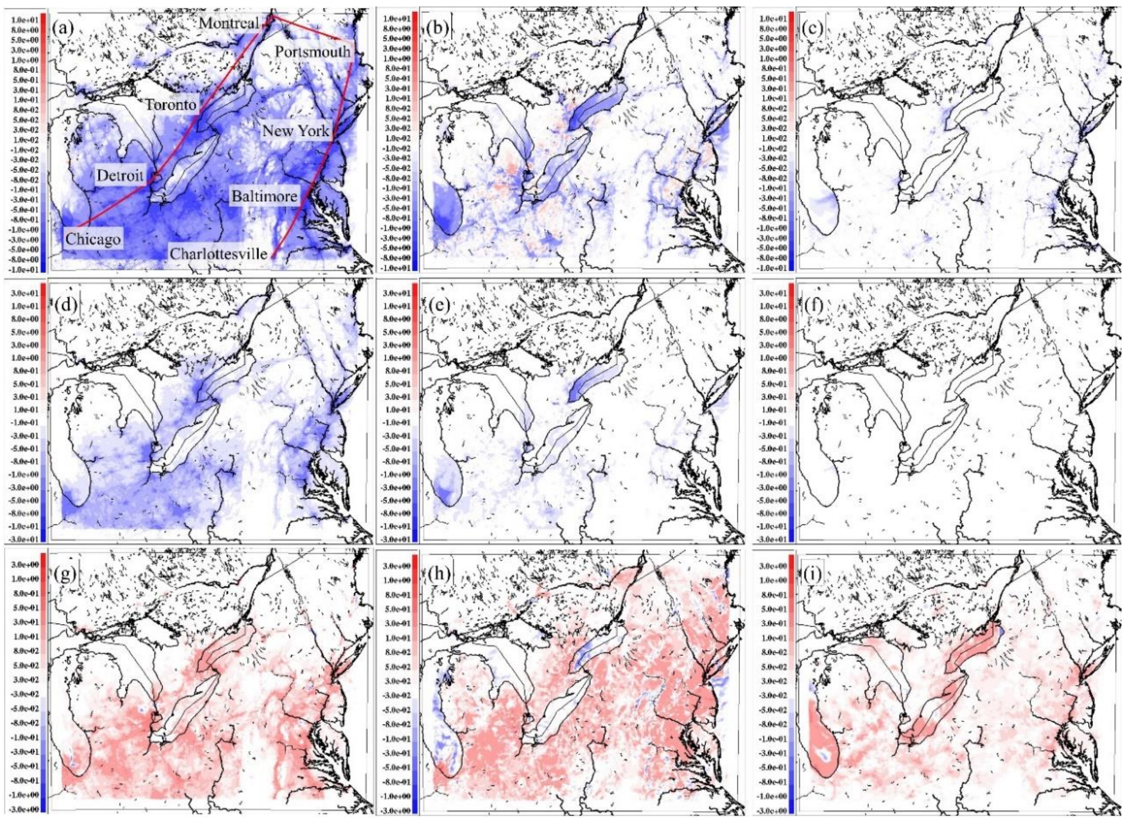

Fig. S6. Difference in 30 day average surface NO_2, PM2.5 and O_3, July 2015, PanAm 2.5km grid cell size domain simulation. Averages are paired at (10, 14, and 22UT) according to species; (a,b,c): ΔNO_2;(ppbv) (d,e,f) ΔPM2.5 (μg m^{-3}); (g,h,i) ΔO_3 (ppbv). Red line in panel (a) indicates position of vertical cross-section shown in Figure S7.

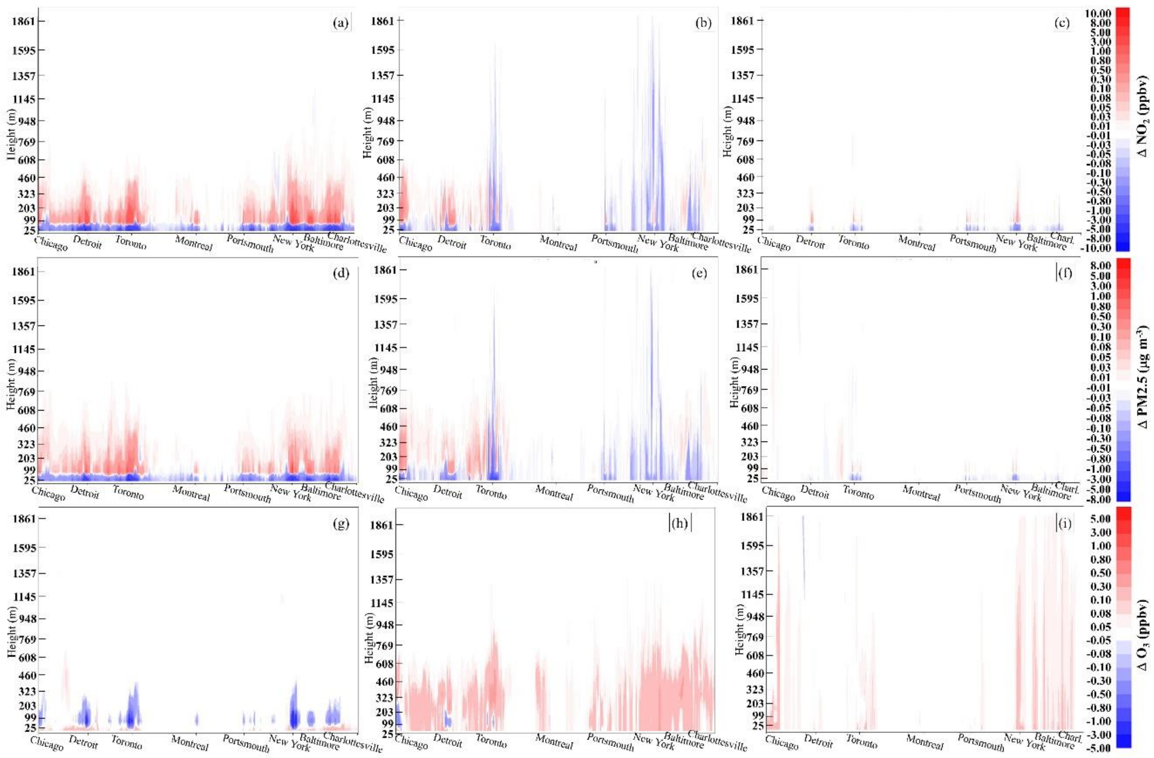

Fig. S7. Vertical cross-sections of concentration differences between major eastern North American cities, July 2015, panels arranged as in Figure S6. Vertical coordinate: unitless hybrid, top-of-scale is approximately 2 km.

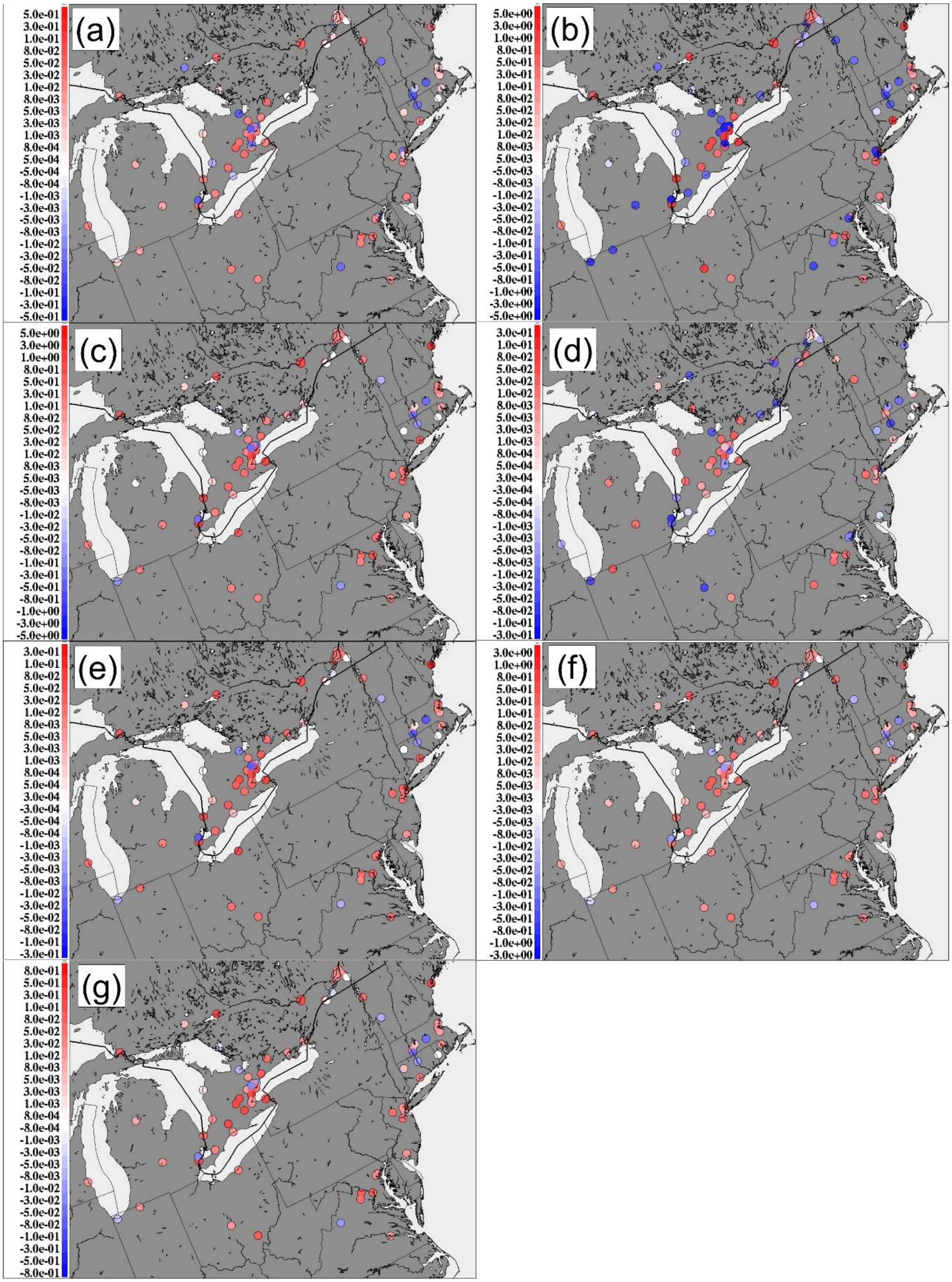

Fig. S8. Change in model NO_2 performance at 94 surface monitoring sites in the PanAM 2.5km domain, July 2015 (ppbv). Colours and panel labels as in Figure S4.

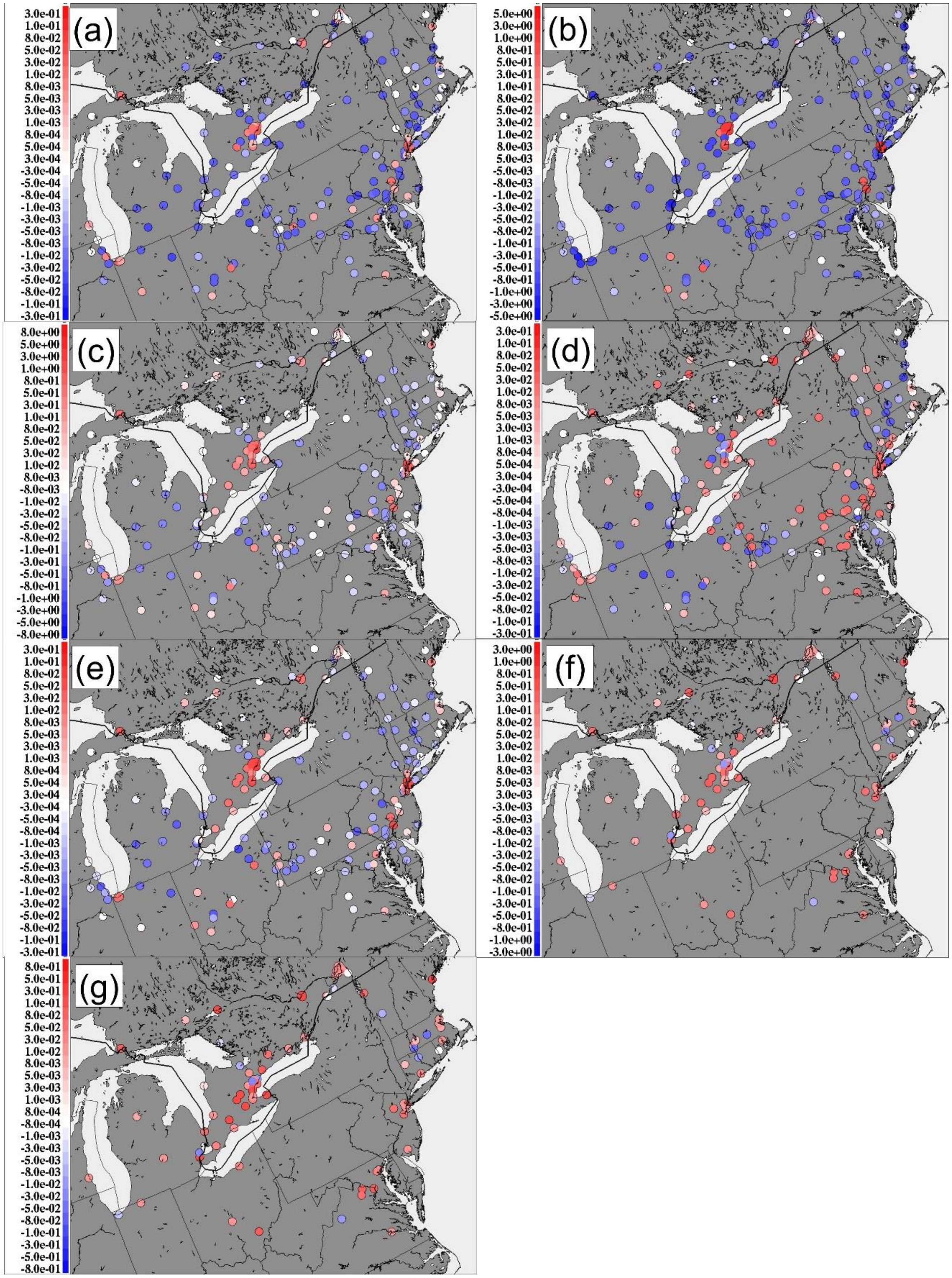

Fig. S9. Change in model PM2.5 performance at 189 surface monitoring sites in the PanAM 2.5km domain, July 2015 (ppbv). Colours and panel labels as in Figure S4.

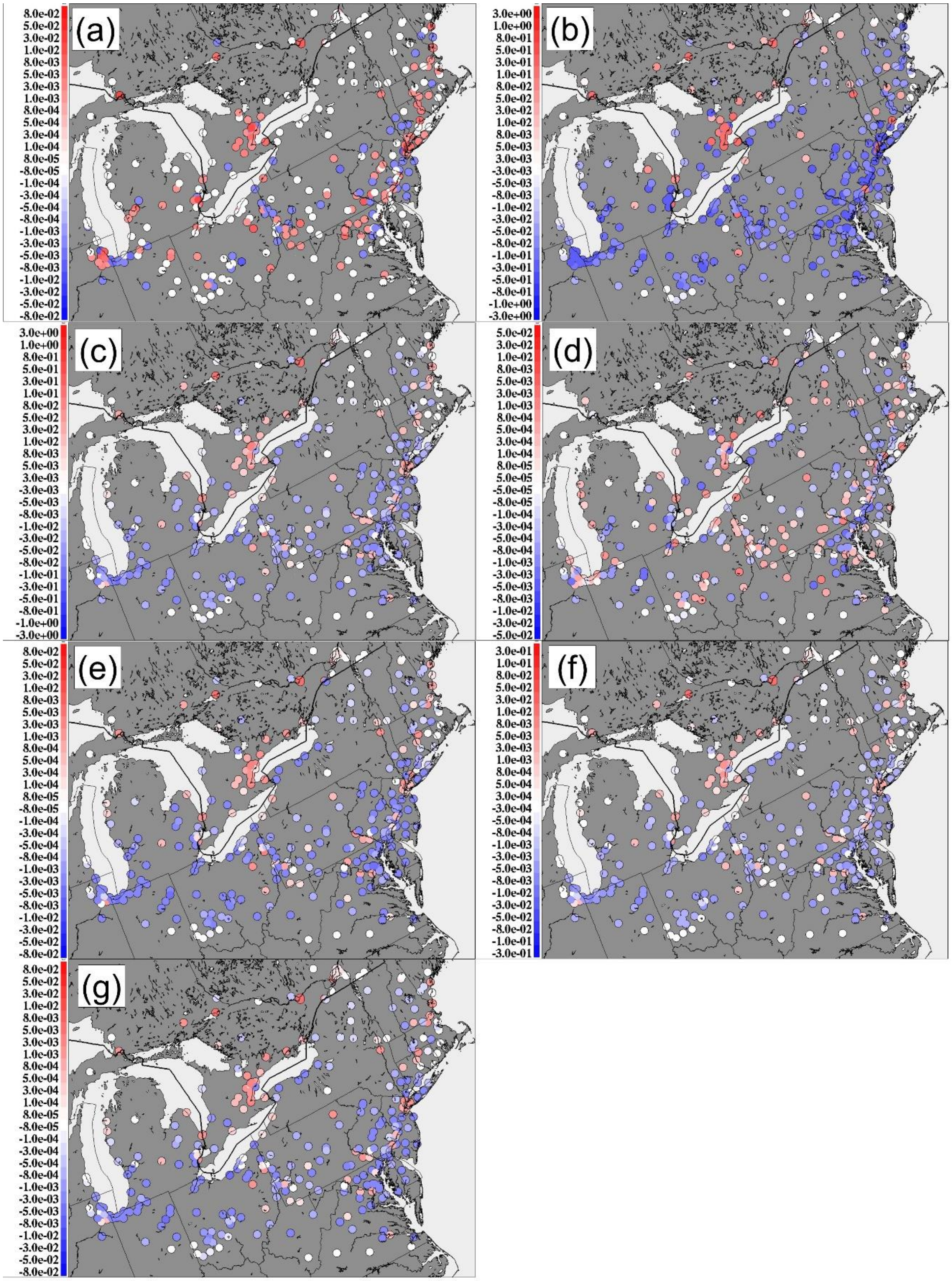

Fig. S10. Change in model O_3 performance at 331 surface monitoring sites in the PanAM 2.5km domain, July 2015 (ppbv). Colours and panel labels as in Figure S4.

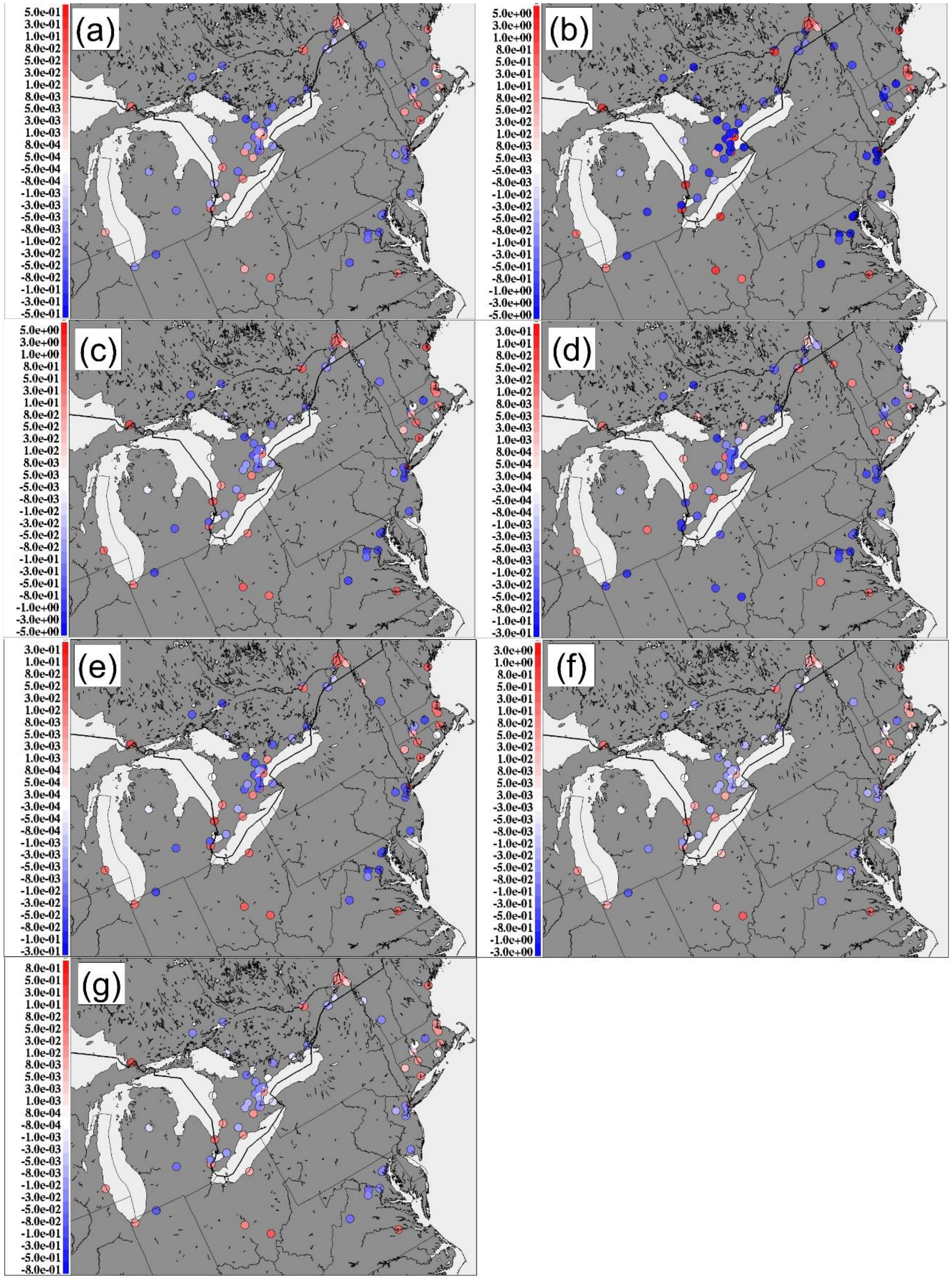

Fig. S11. Change in model NO_2 performance at 94 surface monitoring sites in the PanAM 2.5km domain, January 2016 (ppbv). Colours and panel labels as in Figure S4.

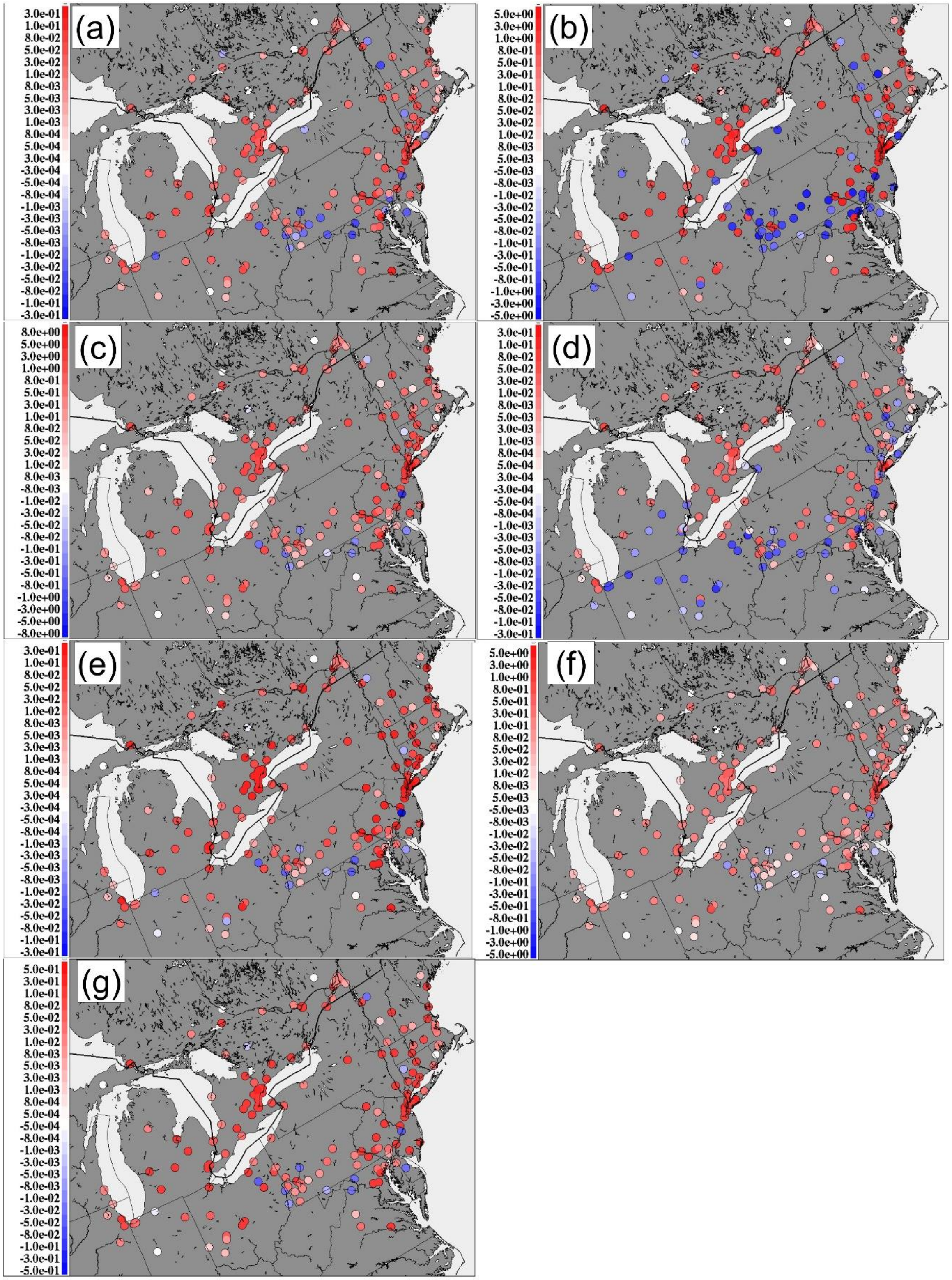

Fig. S12. Change in model PM2.5 performance at 192 surface monitoring sites in the PanAM 2.5km domain, January 2016 (ppbv). Colours and panel labels as in Figure S4.

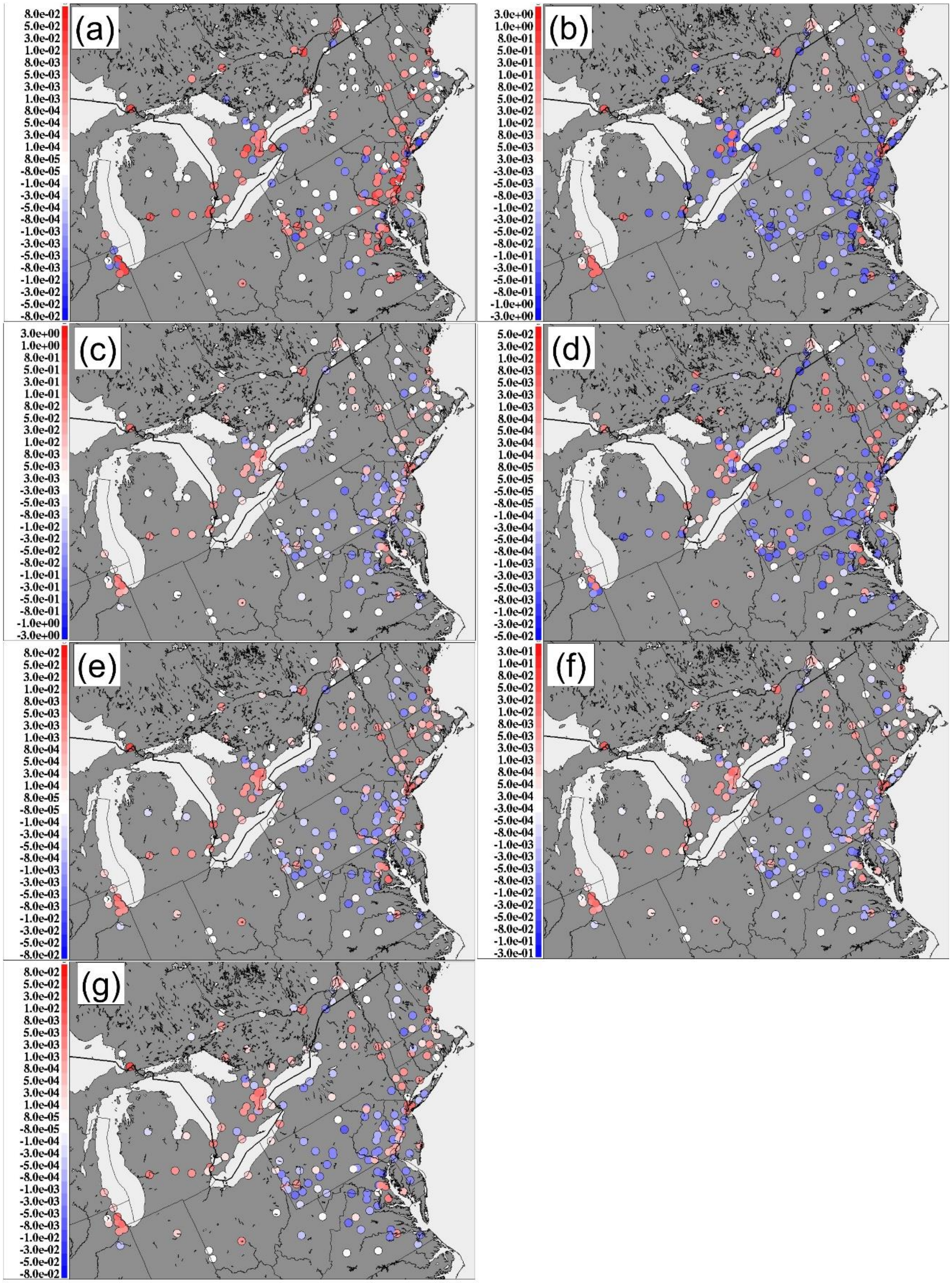

Fig. S13. Change in model O_3 performance at 217 surface monitoring sites in the PanAM 2.5km domain, January 2016 (ppbv). Colours and panel labels as in Figure S4.

Table S1. Statistical metrics used for model performance evaluation.

.

Metric Abbreviation	Formulae (M = model, O = observation)	Meaning	Perfect Score (Range of Scores)
FAC2	$0.5 \leq \frac{M_{\mathrm{i}}}{O_{\mathrm{i}}} \leq 2.0$	Fraction of model-observation pairs for which the model values fall within a factor of two of the observations.	1.0
MB	$MB = \frac{1}{N}\sum_{\mathrm{i}=1}^{N} M_{\mathrm{i}} - O_{\mathrm{i}}$	Mean bias: average of the difference (model – observation) for all data pairs. Negative/positive values indicate model values are lower/higher than observations.	0.0
MGE	$MGE = \frac{1}{N}\sum_{\mathrm{i}=1}^{N} \lvert M_{\mathrm{i}} - O_{\mathrm{i}}\rvert$	Mean Gross Error (aka Mean Absolute Error): average *magnitude* of the difference between model and observations.	0.0
RMSE	$RMSE = \sqrt{\left(\frac{\sum_{\mathrm{i}=1}^{N}(M_{\mathrm{i}} - O_{\mathrm{i}})^2}{N}\right)}$	Root Mean Square Error: standard deviation of differences between model and observation pairs.	0.0
r	$r = \frac{1}{(N-1)}\sum_{\mathrm{i}=1}^{N}\left(\frac{M_{\mathrm{i}} - \bar{M}}{\sigma_{\mathrm{M}}}\right)\left(\frac{O_{\mathrm{i}} - \bar{O}}{\sigma_{\mathrm{O}}}\right)$	Pearson correlation coefficient: a measure of the degree of linear dependence between model and observations.	+1.0
COE	$COE = 1.0 - \frac{\sum_{\mathrm{i}=1}^{N}\lvert M_{\mathrm{i}} - O_{\mathrm{i}}\rvert}{\sum_{\mathrm{i}=1}^{N}\lvert O_{\mathrm{i}} - \bar{O}\rvert}$	Coefficient Of Efficiency: a measure of model accuracy relative to the mean of the observations: a	1.0

		score of zero would indicate that the observed mean is as accurate a predictor as the model values.	
IOA	$IOA = \begin{cases} 1.0 - \frac{\sum_{i=1}^{N}\lvert M_i - O_i\rvert}{2\sum_{i=1}^{N}\lvert O_i - \bar{O}\rvert}, when \sum_{i=1}^{N}\lvert M_i - O_i\rvert \le 2\sum_{i=1}^{N}\lvert O_i - \bar{O}\rvert \\ \frac{2\sum_{i=1}^{N}\lvert O_i - \bar{O}\rvert}{\sum_{i=1}^{N}\lvert M_i - O_i\rvert} - 1.0, when \sum_{i=1}^{N}\lvert M_i - O_i\rvert > 2\sum_{i=1}^{N}\lvert O_i - \bar{O}\rvert \end{cases}$	Index Of Agreement: compares the magnitudes of the model-observation differences to the magnitude of the difference between the observations and their mean.	1.0